Computers and Chemical Engineering 48 (2013) 1–13

Contents lists available at SciVerse ScienceDirect

Computers and Chemical Engineering

journal homepage: www.elsevier.com/locate/compchemeng

Integral formulation of the population balance equation: Application to particulate systems with particle growth

Menwer Attarakih

The University of Jordan, Faculty of Engineering & Technology, Department of Chemical Engineering, 11942 Amman, Jordan

ARTICLE INFO

Article history:
Received 10 March 2012
Received in revised form 29 July 2012
Accepted 1 August 2012
Available online 11 August 2012

Keywords:
Integral population balance
Numerical solution
Mathematical modeling
CQMOM
Particle growth

ABSTRACT

Numerical solution of the population balance equation (PBE) is widely used in many scientific and engineering applications. Available numerical methods, which are based on tracking population moments instead of the distribution, depend on quadrature methods that destroy the distribution itself. The reconstruction of the distribution from these moments is a well-known ill-posed problem and still unresolved question. The present integral formulation of the PBE comes to resolve this problem. As a closure rule, a Cumulative QMOM (CQMOM) is derived in terms of the monotone increasing cumulative moments of the number density function, which allows a complete distribution reconstruction. Numerical analysis of the method show two unique properties: first, the method can be considered as a mesh-free method. Second, the accuracy of the targeted low-order cumulative moments depends only on order of the CQMOM, but not on the discrete grid points used to sample the cumulative moments.

1. Introduction

The population balance equation finds many scientific and engineering applications with mono- and multivariate number density functions. Such applications (not to name but to mention) include multiphase flows and turbulence modeling, aerosol science and kinetic theory and biological and biomedical engineering (Attarakih, Drumm, & Bart, 2009; Favero & Lage, 2012; Fox, 2008, 2009; Hjortso, 2004; John, Angelov, Öncülc, & Thévenin, 2010; Lage, 2011; Majumder, Kariwala, Ansumali, & Rajendran, 2012a, 2012b; Marchisio & Fox, 2005; McGraw, 1997; Piskunov & Golubev, 2002; Raikar, Bhatia, Malone, & Henson, 2006; Ramkrishna, 2000; Rosner, McGraw, & Tandon, 2003; Strumendo & Arastoopour, 2009). Fluid phases which are discrete either at the molecular or particle level can be described by a statistical Boltzmann-type equation, which is called the population balance equation (PBE) (Fox, 2008; Ramkrishna, 2000). The PBE determines the temporal and spatial evolution of particle distribution due to the interactions within the population of particles on the one hand, and the interaction of particles and the continuous phase in which they are imbedded on the another hand (Ramkrishna, 2000). The PBE is a hyperbolic integro-partial differential equation characterized by a nonlinear source term. This source term accounts for various mechanisms with which particles of a specific state can either form or disappear from the system. These mechanisms are discrete and relatively instantaneous compared to the system scale such as particle breakage, aggregation, growth and nucleation (Ramkrishna, 2000). The PBE describing these interactions can describe the system behavior up to any degree of detail. Thus, such population balance models are very suitable for understanding and investigating many single processing units, not to mention, crystallizers, turbulent flame reactors, polymerization reactors, bubble phase reactors, and extraction columns (Abedini & Shahrokhi, 2008; Drumm, Attarakih, Hlawitschka, & Bart, 2010; Motz, Mitrovic, & Gilles, 2002; Rosner, 2006; Wang & Wang, 2007). However; due to their complexity and in the absence of general analytical solution, these population balance models are hardly used in flowsheeting programs to simulate whole plants made up of many unit operations and thus they cannot be used as design models or in model predictive control (Abedini & Shahrokhi, 2008; Cameron, Wang, Immanuel, & Stepanek, 2005; Chiu & Christofides, 2000). Moreover, computational fluid dynamics (CFD) has been used with great success to explore the detailed flow fields in a very complex real geometry with an obvious need to detailed modeling of the dispersed phase. The excessive computational burden placed by including the population balance equation as a dispersed phase modeling tool limits such benefits even with super speed computers (Drumm et al., 2010; Fox, 2008; Motz et al., 2002; Rosner, 2006; Tiwari, Drumm, Attarakih, Kuhnert, & Bart, 2008). Therefore, there is an engineering need to have a simple reduced model for discrete phases, without losing the detailed description of the phenomena inherently embedded in the population balance equation. One of the popular model formulations is the transformation of the population balance equation into a set of self-contained integral equations that describe the moments' evolution

E-mail addresses: attarakih@yahoo.com, m.attarakih@ju.edu.jo

0098-1354/$ – see front matter © 2012 Elsevier Ltd. All rights reserved.
http://dx.doi.org/10.1016/j.compchemeng.2012.08.001

Nomenclature

G	particle growth rate (m/s)
G_0	particle growth rate constant (model dependent)
J	Jacobian matrix defined by Eq. (8)
L	number of points used in fixed grid
M	number of points used in moving grid
N	number of time integration steps
N_q	number of quadrature points
P	matrix defined by Eq. (5)
r	order of cumulative moments
t	time (s)
$w(x)dx$	number concentration ($1/m^3$) in the range x, $x+dx$
x	particle size (m)
x_{min}, x_{max}	minimum and maximum particle size (m)
z	spatial coordinate

Greek symbols

α	as defined by equation Eq. (9)
$\beta(x\|x')dx$	number of daughter particle produced by breakage of mother particle of size x' in the range x, $x+dx$
Γ	breakage frequency (1/s)
γ	as defined by Eq. (45)
δ	Kroneker delta
ζ	cumulative quadrature nodes as defined by Eq. (11)
θ	minmod limiter parameter
λ	quadrature weights as defined by Eq. (13)
μ	moments of $w(x)$
σ, σ'	standard deviations defined by Eqs. (12) and (19)
ψ	aggregation frequency (m^3/s)

of the particle size distribution. In general, these methods belong to the moment transformation of the population balance equation at the expense of destroying the distribution itself (Drumm et al., 2010; Lage, 2011; Marchisio & Fox, 2005; McGraw, 1997; Piskunov & Golubev, 2002; Ramkrishna, 2000). In contrast to the classical method of moments, where the closure problem is overcome by a priori assumed distribution or simplified kernel functions (Diemer & Olson, 2002; Hulburt & Katz, 1964; Ramkrishna, 2000), the Quadrature Method Of Moments (QMOM) provides not only an efficient closure to the moment problem, but also an extremely efficient Gauss-like integration quadrature. For critical evaluation and improvements in the QMOM literature, the reader can consult Grosch, Briesen, Marquardt, and Wulkow (2007), Attarakih et al. (2009) and Lage (2011). The QMOM is based on the known low-order moments of the weight function (here in the population balances equation it is the unknown distribution) and requires only a few nodes (two or three) to converge, even for sharply changing integrands. The QMOM or the moment transformed population balance equations are motivated in general by the degree of details required by the physical model. This is because the calculation of most average physical properties of the particulate phase does not require a full knowledge of the size distribution. This is in particular true for properties most relevant to engineering applications such as mean particle size, mean surface area, and average dispersed phase holdup (Attarakih, Bart, & Faqir, 2006; Drumm et al., 2010; Majumder et al., 2012a; Piskunov & Golubev, 2002). However; the major drawback of the moment methods in general and the QMOM in particular is their inability to reconstruct the particle size distribution (PSD). The PSD plays a decisive role in the determination of the physicochemical and mechanical product properties made of particulate systems (Cameron et al., 2005; Chiu & Christofides, 2000; John et al., 2010; Majumder et al., 2012a). Recent advances and development in online measurements and control provide real-time access to system parameters, which are estimated, based on the whole size distribution (Abedini & Shahrokhi, 2008; Cameron et al., 2005; Chiu & Christofides, 2000; Schmidt, Simon, Attarakih, & Bart, 2006; Mickler, Didas, Jaradat, Attarakih, & Bart, 2011).

Therefore, in such applications the need for the full particle size reconstruction from its moments is obvious, where rigorous attempts had appeared in the last decade to resolve this problem (Attarakih et al., 2006; Diemer & Ehrman, 2005; Diemer & Olson, 2002; John, Angelov, Öncülc, & Thévenin, 2007; John et al., 2010; Mnatsakanov & Hakobyan, 2009). Diemer and Olson (2002) presented a non-linear regression method based on the expansion of the solution in a set of orthogonal basis functions of the PSD. A priori idea about the PSD distribution is needed to facilitate the identification of a suitable set of orthogonal functions. Diemer and Ehrman (2005) used a modified gamma functions to reconstruct the PSD in a pipeline agglomerator design. In their numerical experiments, at least the first 10 moments of the distribution are needed to get acceptable reconstructions. Attarakih et al. (2006) used coupled QMOM and the first four terms of the Laguerre polynomial, which are weighted by the gamma function (Hulburt & Katz, 1964) to reconstruct the cumulative distribution function. The numerical results are fairly accurate (using only the first three low-order moments of the distribution) and are close to those predicted using the fixed-pivot technique (Ramkrishna, 2000). John et al. (2007) investigated rigorously the PSD reconstruction from its low-order moments, where they addressed the theoretical and practical difficulties in solving the ill-posed inverse moment problem. They introduced a spline-based reconstruction method, which does not require a prior knowledge of the PSD. In a subsequent publication, John et al. (2010) presented an adaptive spline-based reconstruction method, which they used to reconstruct bimodal PSD as a result of direct simulation of a crystallizer process. The base of this algorithm is the dynamic positioning of the spline interpolating polynomial nodes. The adaptive algorithm showed good improvements in the reconstruction of distributions with a sharp changing shape; however, with lack of positiveness near sharp peaks. This ill-posedness and uniqueness problems of the reconstructed PSD are still open problems, which are addressed by Mnatsakanov and Hakobyan (2009) and John et al. (2007, 2010). John et al. (2007) concluded that "*It is indeed extremely difficult from a theoretical point of view as well as from a practical point of view to find an accurate and relatively fast method which can be applied to all scientific areas*".

On the other hand, distribution reconstructing methods used in the numerical solution of the population balance equation can be categorized into two main groups: sectional methods (Attarakih et al., 2009; Gelbard & Seinfeld, 1980; Kumar & Ramkrishna, 1996; Majumder, Kariwala, Ansumali, & Rajendran, 2010; Ramkrishna, 2000; Smooke, McEnally, Pfefferle, Hall, & Colket, 1999) and methods that are based on the series expansion of the number density function using a complete set of orthogonal trial functions (Hamilton, Curits, & Ramkrishna, 2003; Ramkrishna, 2000; Strumendo & Arastoopour, 2006). Sectional methods represent a simple and straight forward black box solver for the PBE in general; however, with an increasing computational load. This is in particular, when accurate integral properties are to be estimated (Attarakih et al., 2009; Kumar & Ramkrishna, 1996; Majumder et al., 2010, 2012a, 2012b; Xiong & Pratsinis, 1993). Among this category, one can distinguish between internally consistent and inconsistent sectional methods. In contrast to internally inconsistent sectional methods (e.g. simple finite difference or finite volume schemes), internally consistent sectional methods guarantee the reproduction of selected integral low order moments of the population density function (Kumar & Ramkrishna, 1996; Ramkrishna, 2000). This is because these low-order moments derived from the discrete population balance equation are internally consistent with

those derived from the continuous population balance equation (Attarakih et al., 2009; Kumar & Ramkrishna, 1996; Ramkrishna, 2000). The connection between the internally consistent sectional methods and the QMOM is uncovered by Attarakih et al. (2009) and Attarakih (2010), where the distribution reconstruction is realized using the Sectional Quadrature Method Of Moments (SQMOM). The SQMOM provides a hierarchy for solving the PBE, where the distribution accuracy is decoupled from that of the numerical evaluation of the integral quantities. As Attarakih et al. (2009) pointed out; the SQMOM is extended recently to the Direct Quadrature Method Of Moments (SQMOM) and is called SDQMOM (Bruns & Ezekoye, in press). Like any sectional method, the SQMOM is expected to exhibit numerical diffusion across the cells' boundaries when applied to particle growth problems. This is a typical problem when hyperbolic conservation laws are solved numerically (Kumar & Ramkrishna, 1996; Kurganov & Tadmor, 2000).

The second group depends on using series expansion of the number density function with certain trial functions. Hamilton et al. (2003) used the Hermite polynomials as basis functions in the series expansion, while Strumendo and Arastoopour (2006) used Legndre polynomials. The coefficients of expansion in the Hermite series are found using the method of orthogonal collocation. The parameters of the lognormal distribution appearing in the expansion are found by additional set of moment equations. Strumendo and Arastoopour (2006) estimated the coefficients of expansion in terms of the low-order moments of the distribution, which results in a set of moment equations. Despite the accuracy of these methods, they have two common drawbacks that limited their applications in practical problems. The first drawback is the complex source terms in the population balance equation due to either coordinate or domain transformation. The second one is the appearance of many single and double integrals in the source terms, which call for adaptive numerical integration, especially when the number density function becomes too sharp. This increases the computational time when compared to the fixed pivot technique (Hamilton et al., 2003). Additionally, the integration domain transformation used by Strumendo and Arastoopour (2006) results in a moving boundary problem, which is proved to be problem dependent. Recently, Lage (2011) presented a general review guide for the recent numerical methods in solving the population balance equation. As a result, he derived the QMOM from a weighted residual method through introducing the dual quadrature method of generalized moments (DuQMoGeM), which is based on weighted residual formulation. In this method, a quadrature rule of high accuracy is used to evaluate the integrals that are required as a closure of the system of equations for the generalized moments. The moment equations were integrated using a high order fixed-point Gaussian quadrature. In another publication, Favero and Lage (2012) showed how the DuQMoGeM can be extended to solve the multivariate PBE. The proposed methodology consists of using automatic integration packages in the DuQMoGeM to eliminate the integration errors in the evaluation of the moments of the population balance equation.

Note that the foregoing review highlights the great advantage of the QMOM as a fast population balance solver and the advantage of sectional methods as a distribution reconstructing methods. This is in particular, sectional methods where the integral quantities are not very sensitive to the reconstructed distribution itself like the moving pivot technique (Kumar & Ramkrishna, 1996), the SQMOM (Attarakih et al., 2009) and the SDQMOM (Bruns & Ezekoye, in press). Therefore, the sought numerical scheme should combine the advantages of quadrature and sectional methods, especially the elimination of numerical diffusion in growth problems and provides an efficient closure for the unclosed integrals.

This work presents a method, which obviously fulfills the aforementioned requirements without restricting the number density function to anyone of the traditional functional forms like the log-normal or modified gamma distributions or even requires trial functions. As a result of applying cumulative rather than global moment transformation, an integral PBE with an unclosed source term is obtained. The present method uses a hierarchical novel formulation of the population balance equation, in which the rth (with respect to particle property space) cumulative distribution is reconstructed from its cumulative sections. Here, the rth moment of the distribution is function of the particle internal property and evolves in time and physical space through a set of transport equations. Since the rth cumulative moment at any grid point along the particle property space is not expected to affect the global moments, the number and structure of the grid points are not going to affect the accuracy of the cumulative integration quadrature. The unknown distribution appearing as an integrand is used as the weight function in the Gauss–Christoffel quadrature formula (Gautschi, 1968). The continuous variation of the abscissa and weights (along the particle property space) of this quadrature are obtained using closed analytical forms of a two-node quadrature. For the nth-node quadrature, the standard product difference algorithm (PDA) (McGraw, 1997) is extended to a continuous cumulative quadrature. Due to the combination of the cumulative (rather than global moments of the population) moments with the QMOM, the method is given the name: Cumulative QMOM or shortly CQMOM. The advantage of the CQMOM over the SQMOM (Attarakih et al., 2009) is its internal consistency in solving particle growth problems. Although the integral PBE for simultaneous particle growth, breakage and aggregation is present in this paper, examples of only particle growth is considered here since the ideas for the case of integral population balance of particle breakage and coagulation were published (Attarakih & Bart, 2012; Attarakih, Jaradat, Hlawitschka, & Bart, 2011). Therefore, in this paper, the focus is only on cases of the homogeneous one-dimensional PBE with particle growth.

2. The Cumulative Quadrature Method Of Moments (CQMOM)

Let $\omega(x;z,t)$ be a nonnegative integrable function on the interval $[a, b]$ such that

$$\int_{a=0}^{x} w(\zeta;.)d\zeta > 0, \quad x \in [a,b] \tag{1}$$

and all its cumulative moments exists. Note that the dependency of $w(x;.)$ on the external coordinates: space (z) and time (t) are replaced by a dot for simplicity. Now, let the cumulative moments of $w(x;.)$ be defined as:

$$\mu_r(x;.) = \int_{a=0}^{x} \zeta^r w(\zeta;.)d\zeta, \quad r = 0,1,2\ldots 2N_q-1 \tag{2}$$

and redefine the Gauss–Christoffel quadrature (Gautschi, 1968) in terms of $\mu_r(x;.)$:

$$\mu_r(x;.) = \sum_{j=1}^{N_q} \lambda_j(x;.)[\zeta_j(x;.)]^r, \quad r = 0,1,\ldots 2N_q-1 \tag{3}$$

where $\zeta_j(x;.) \in [0,x]$ are the quadrature nodes (abscissa) along the particle property space (chosen here to be the particle diameter), $\lambda_j(x;.)$ are the nonnegative quadrature weights associated with the weight function $w(x;.)$ and N_q is the number of quadrature points. The above integration quadrature is exact for integrands that are polynomials of degree at most $2N_q-1$. Note that in contrast to the QMOM, the CQMOM is formulated using nodes and weights that are functions of the particle property space. This quadrature has continuous nodes and weights as long as the cumulative moments from which they are constructed are continuous. The Gauss–Christoffel

quadrature can be viewed as a special case when the limits of integration given by Eq. (1) are fixed over the interval $[a, b]$. Note that $\mu_0(x) = W(x)$, which is the cumulative distribution of $w(x)$ and the other cumulative moments (for $r = 1, 2, \ldots 2N_q - 1$) are all monotone and at least right continuous functions. These functions satisfy two important properties:

$$\mu_r(0) = 0, \lim_{x\to\infty} \frac{\partial \mu_r(x)}{\partial x} = 0 \tag{4}$$

These properties help in eliminating the so-called finite domain error during the solution of the population balance equation and force the numerical schemes to be conservative (with respect to x).

To find the quadrature nodes and weights given by Eq. (3) at any point x along the particle property space, the general approach consists of constructing a system of orthogonal polynomials with respect to the weight function $w(x;.)$. The quadrature nodes are then the zeros of these orthogonal polynomials with respect to the weighing function. The weights are found in a number of possible ways, in terms of these orthogonal polynomials (Gautschi, 1968; Gordon, 1968). Unfortunately, finding roots of polynomials is a well-known ill-posed problem and there is no guarantee to get real nodes and weights or even force their positivity, which is a physical necessity (Gordon, 1968; Piskunov & Golubev, 2002). As an alternative, a robust procedure based on the product difference algorithm (PDA) is suggested by Gordon (1968). This algorithm is first used by McGraw (1997) as an effective tool to calculate the weights and the abscissas from a given set of low-order moments over the interval $(0, \infty)$. Here the PDA is adapted to accommodate the cumulative sectional moments given by Eq. (3) with the help of the theoretical guidelines presented by Gautschi (1968). The first step is the construction of a matrix $P(x;.)$ with components $P_{i,j}(x;.)$ starting from the cumulative moments. The components in the first, second and jth columns of the matrix $P(x;.)$ are:

$$P(x;.) = \left(\begin{bmatrix} \delta_{i,1} \\ i \in 1, 2 \ldots 2N_q + 1 \end{bmatrix} \quad \begin{bmatrix} p_{i,1}(x) = (-1)^{i-1}\mu_{i-1}(x) \\ i \in 1, 2, \ldots 2N_q + 1 \end{bmatrix} \quad \begin{bmatrix} p_{i,j}(x) \\ j \in 3, 4, \ldots 2N_q + 1 \\ i \in 1, 2, \ldots 2N_q + 2 - j \end{bmatrix} \right) \tag{5}$$

where

$$p_{i,j}(x) = P_{1,j-1}P_{i+1,j-2} - P_{1,j-2}P_{i+1,j-1} \tag{6}$$

and the nodes and weights are now given by:

$$\begin{aligned} &\zeta(x;.) = eigenvalues(J(x;.)) \\ &\lambda_j(x;.) = \mu_0(x;.)(v_{j,1}(x;.))^2, \quad j = 1, 2 \ldots 2N_q \end{aligned} \tag{7}$$

where $J(x;.)$ is the Jacobian matrix with elements that are given by:

$$J(x;.) = \begin{cases} J_{i+1,i} = -\sqrt{\alpha_{2i}(x)\alpha_{2i-1}(x)}, & i = 1, 2, \ldots N_q - 2 \\ J_{i,i} = \alpha_{2i}(x) + \alpha_{2i-1}(x), & i = 1, 2, \ldots N_q - 1 \\ J_{i,i+1} = -\sqrt{\alpha_{2i}(x)\alpha_{2i-1}(x)}, & i = 1, 2, \ldots N_q - 2 \end{cases} \tag{8}$$

$$\alpha(x;.) = \begin{cases} \alpha_1 = 0 \\ \alpha_i(x) = \dfrac{P_{1,i+1}(x;.)}{P_{1,i}(x;.)P_{1,i-1}(x;.)}, & i = 2, 3 \ldots 2N_q \end{cases} \tag{9}$$

Note that $v_{j,1}(x)$ is the first component of the jth normalized eigenvector of the Jacobian matrix $(J(x;.))$ and $\delta_{i,j}$ is the Kronecker delta. Moreover, it is clear that $\lambda_j(x;.)$ are always positive by virtue of Eq. (6) and since the eigenvalues should satisfy $\zeta_j(x;.) \in [0, x]$, then $\zeta_j(x;.) > 0, \forall j$, where $x > 0$ and $w(x;:)$ is a positive semi-definite function, which satisfies $w(x;:) \geq 0, \quad \forall x \geq 0$ (Gordon, 1968; Sasvari, 1994).

2.1. The two-unequal and equal weight quadratures

Note that the Jacobian matrix $(J(x;.))$ is a real $(\alpha \geq 0)$ and symmetric tridiagonal matrix that is well-conditioned. This allows the eigenvalues and the corresponding eigenvectors to be accurately evaluated (Gordon, 1968). In this section, the number of quadrature points in Eq. (3) is restricted to two, which allows us to find an analytical solution to the eigenvalue problem: $|J(x;.) - \zeta I| = 0$, where I is the identity matrix. The 2×2 symmetric matrix resulting from Eqs. (5), (6), (8) and (9) is given by:

$$\begin{vmatrix} \hat{\mu}_1(x) - \zeta(x) & -\sigma(x) \\ -\sigma(x) & (\sigma^2(x)/\hat{\mu}_1(x) + \alpha_4(x)) - \zeta(x) \end{vmatrix} = 0 \tag{10}$$

The formal solution of this eigenvalue problem results in the following set of particle size dependent nodes and weights:

$$\zeta_{1,2}(x) = \frac{1}{2}\left(\frac{\hat{\mu}_3(x) - \hat{\mu}_1(x)\hat{\mu}_2(x)}{\sigma^2(x)}\right) \mp \sqrt{\left(\frac{1}{2}\frac{\hat{\mu}_3(x) - \hat{\mu}_1(x)\hat{\mu}_2(x)}{\sigma^2(x)}\right)^2 - \hat{\mu}_1(x)\alpha_4(x)} \tag{11}$$

where

$$\alpha_4(x) = \frac{\hat{\mu}_1(x)\hat{\mu}_3(x) - \hat{\mu}_2^2(x)}{\hat{\mu}_1(x)\sigma^2(x)}, \quad \sigma^2(x) = \hat{\mu}_2(x) - \hat{\mu}_1^2(x) \tag{12}$$

$$\lambda_{1,2}(x) = \mu_0(x)\left(\frac{\sigma(x)}{\zeta_m(x) - \zeta_{1,2}(x)}\right)^2 \frac{1}{1 + (\sigma(x)/[\zeta_m(x) - \zeta_{1,2}(x)])^2} \tag{13}$$

and

$$\zeta_m(x) = \hat{\mu}_1(x), \quad \hat{\mu}_r(x) = \frac{\mu_r(x)}{\mu_0(x)} \tag{14}$$

In the above equations, α_4 is derived from Eq. (9) and σ^2 is the population variance for particles of size less than or equal to x.

The above analytical expressions reflect many important properties of the CQMOM in general and the QMOM in particular. First, the quadrature two weights are always positive as given by Eq. (13) and they do not exist when the quadrature nodes tend to the mean particle size, which is given by Eq. (14). This special case occurs when the particle size distribution becomes a perfect Dirac delta function located at the mean value $\zeta_m(x)$. This justifies the breakdown of the QMOM or the DQMOM as reported by Marchisio and Fox (2005) and Su, Gu, Li, Feng, and Xu (2008). The second property is clear by finding the arithmetic mean of the particle size distribution using Eq. (11):

$$\bar{\zeta}(x) = \frac{1}{2}\left(\frac{\hat{\mu}_3(x) - \hat{\mu}_1(x)\hat{\mu}_2(x)}{\sigma^2(x)}\right) \tag{15}$$

As a direct consequence of this result, the nodes given by Eq. (11) can be viewed as fluctuation (symmetric) of the particle size around its arithmetic mean at any given point x. Another important constraint on the evolution of the cumulative moments follows directly from the second term on the right hand side of Eq. (11), which avoids the occurrence of complex weights and abscissa. This can be

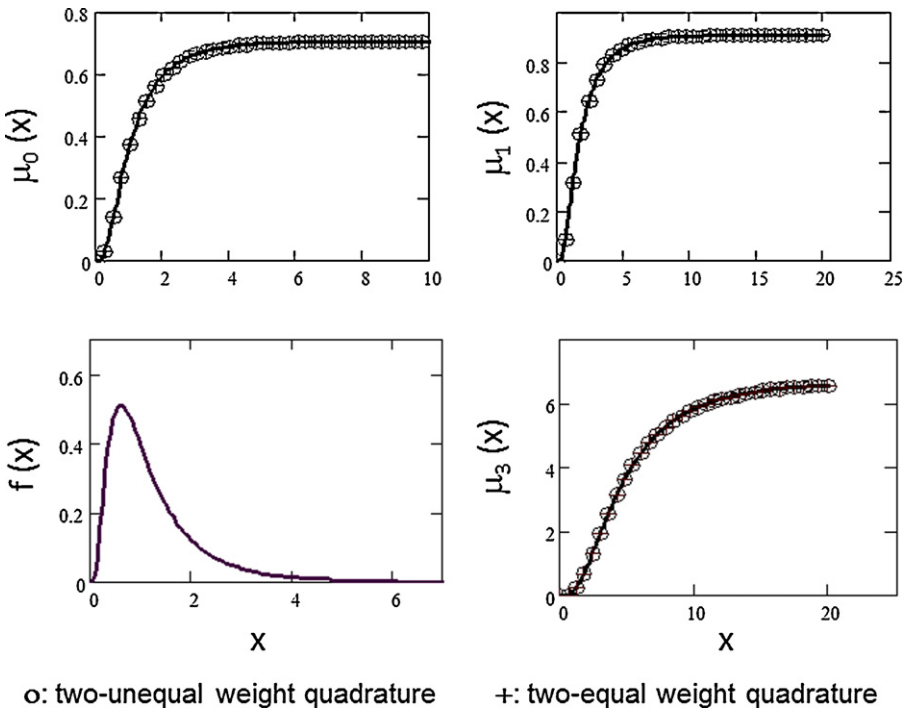

Fig. 1. Comparison between the exact (solid lines) and reconstructed cumulative moments along particle size. The exact cumulative moments are those of lognormal distribution function $f(x)$ with mean and standard deviation equal to 0.0 and 1.0, respectively, using the two-unequal and equal weight quadratures.

realized by noting that the quantity under the square root is always positive; that is, $\left[\bar{\zeta}(x)\right]^2 - \hat{\mu}_1(x)\alpha_4(x) \geq 0$, which follows from the fact that the cumulative nodes are eigenvalues of a real and symmetric Jacobain matrix.

To test the reliability of the cumulative two-unequal weight quadrature for reproducing the input cumulative moment vector ($\mu(x)$), a standard test is performed as shown in Fig. 1 using the exact cumulative moments of the lognormal normal distribution function. It is clear how the input cumulative moment vector is accurately reproduced using the reconstruction formula given by Eqs. (3) and (11)–(14). Here, the particle property space is sampled uniformly according to the partition: $x_i = 0.5i$, $i = 1, 2 \ldots 14$.

Despite the reliability of the two-unequal weight quadrature derived above, it collapses when the population function tends to a monosize distribution or it suffers from serious round off errors when the distribution becomes very narrow. This problem is inherited from the PDA itself due to the appearance of quantities suffering from loss of significance like $\hat{\mu}_1(x)\hat{\mu}_3(x) - \hat{\mu}_2^2(x)$ and $\sigma^2(x)$. To overcome the breakdown of the two-unequal weight quadrature when $\sigma(x) \to 0$, we propose the two-equal weight quadrature as a possible alternative. In addition, the equal-weight quadrature formulas are proved to minimize the *root mean-square round off error* in a statistical sense (Isaacson & Keller, 1994). So, the idea behind using equal-weight quadratures is not new and stemmed from the theory of Gauss quadrature to reduce round off errors (Isaacson & Keller, 1994). Now, the cumulative quadrature given by Eq. (3) with equal weights can be written as:

$$\mu_r(x;.) = \frac{\mu_0(x;.)}{N_q}\sum_{j=1}^{N_q}[\zeta_j(x;.)]^r, \quad r = 0, 1, \ldots 2N_q - 1 \tag{16}$$

It is obvious that the weights are now uniform and they are equal to $\lambda_j(x) = \mu_0(x)/N_q$. If we use only two-node quadrature, then we are left with only two degrees of freedom to find these nodes by solving the polynomial equation given by Eq. (16). Moreover, since the internal particle property space is taken here as particle diameter, a feasible choice of the cumulative moments is $\mu_1(x)$ and $\mu_3(x)$. The choice of the third order moment is for the purpose of mass conservation. The second order moment will be estimated with reasonable accuracy since the uniform integration quadrature is interpolatory with precision at least N_q (Isaacson & Keller, 1994). Solving Eq. (16) for the polynomial roots one can easily get the following two nodes:

$$\zeta_{1,2}(x) = \hat{\mu}_1(x) \mp \sigma'(x) \tag{17}$$

$$\sigma'(x) = \frac{1}{\sqrt{3}}\sqrt{\frac{\hat{\mu}_3(x)}{\hat{\mu}_1(x)} - \hat{\mu}_1^2(x)} \tag{18}$$

Note that the two quadrature nodes given by Eq. (17) are now symmetric about the mean of the particle size in the interval [0, x], which is in agreement with the uniform quadrature theory (Isaacson & Keller, 1994). Moreover, the estimation of variance of the particle population of size less than or equal to x is given by Eq. (18). The second cumulative moment is predicted by combining Eqs. (16)–(18). After straight forward algebraic manipulations, the second cumulative moment is given by:

$$\hat{\mu}_2(x) = (\hat{\mu}_1(x))^2 + \sigma'(x) \tag{19}$$

Fig. 1 compares the reproduced cumulative moments using the two-equal weight quadrature with exact input moments generated from the lognormal distribution density function. Like the unequal weight quadrature, the two-equal weight quadrature reproduced exactly the input cumulative moment vector. Moreover, the two-equal weight quadrature given by Eqs. (17) and (18) does not collapse when the distribution tends to a monosize distribution. This is because as the variance tends to zero, $\sigma'(x)$ given by Eq. (18) tends also to zero and the two quadrature nodes (Eq. (17)) become identical and equal to the location of the Dirac delta function at $x_{1,2} = \hat{\mu}_1$. In this special case the two-equal weight quadrature can reproduce exactly all the moments of the monosize distribution. Su et al. (2008) tried to alleviate partially this problem by adjusting the quadrature nodes based on reconditioning the linear system used

to solve for quadrature nodes in the Direct Quadrature Method Of Moments (DQMOM).

3. Integral formulation of the population balance equation

The population balance equation describes the evolution of dispersed phase, which is surrounded by a continuous phase. The dispersed phase (depending on application) consists of solid particles, gas bubbles, liquid droplets or even biological cells (Ramkrishna, 2000). Particles in a given population interact not only with each other, but also with the surrounding continuous phase, which in many times deforms these particles and leads to breakage and aggregation events, growth or even nucleation (Cameron et al., 2005; Ramkrishna, 2000; Schmidt et al., 2006). During particles' residence time in a given homogeneous space, the internal states of these particles undergo physical or chemical changes. In general, the inherent properties of a particle (such as size, concentration, and temperature) are referred to as internal states or coordinates. This is to distinguish them from the particles' spatial position and time, which are referred to as external coordinates. The distribution of particles in state space is described by a number concentration function, which can be defined based on the specific internal state of the concerned system. Although it is not a restriction, we will restrict the particle internal state to only one variable; namely, the particle size x. Accordingly, the number of particles per unit volume of a homogenous space is $w(x;t)dx$ and its evolution along particle size and time is given by the following population balance equation (Attarakih et al., 2006; Ramkrishna, 2000):

$$\frac{\partial w(x;t)}{\partial t} + \frac{\partial (Gw)}{\partial x} = S_b(w) + S_c(w) \tag{20}$$

$$S_b(w) = -\Gamma(x;\varphi)w(x;t) + \int_x^\infty \Gamma(x';\varphi)\beta(x|x')w(x';t)dx' \tag{21}$$

$$S_c(w) = \frac{1}{2}\int_0^x \left(\frac{x}{\eta}\right)^2 \psi(\eta,u,\varphi)w(u;t)w(\eta;t)du - w(x;t)\int_0^\infty \psi(x,u,\varphi)w(u;t)du \tag{22}$$

where $\eta(x,u) = \sqrt[3]{x^3-u^3}$, $\Gamma(x;t,\varphi)$ is the particle breakage frequency, which is usually function of particle size, dispersed phase holdup (φ) and energy dissipation, $\beta(x|x')$ is the distribution of daughter particles broken from a mother particle of size (x') and should satisfy the total number and mass constraints (Ramkrishna, 2000). The aggregation frequency between two particles of sizes x and u is $\psi(x,u;\varphi)$, which usually expressed as a product of two functions: the aggregation frequency and the aggregation efficiency. The latter expresses the probability of successful collisions between two particles of sizes x and u, which is usually function of the turbulent energy fluctuations in the continuous phase (Drumm et al., 2010). The first two terms on the left hand side of Eq. (20) are the rate of accumulation of particles and the particle growth along particle size x. The growth rate $G(x;c)$ is generally function of particle size and the continuous phase variable c. The two terms on the right hand side are the source terms of breakage and aggregation, which are functional of the particle size function $w(x;t)$ and are given by Eqs. (21) and (22). The first term on the right hand side of Eq. (21) is the rate of disappearance of particles of size x due to breakage, while the second term represents the total number of particles formed due to breakage of mother particle of size x' into daughter particles of size x. The two terms on the right hand side of Eq. (22) are the rate of disappearance and formation of particles due to aggregation events.

Note that the number concentration function $w(x;t)$ is a differential rather than cumulative distribution function, which is positive definite function in terms of particle diameter (see Section 2). In many applications involving population balance problems, it is often desirable to work with the cumulative distribution function. A famous example is the solution of the inverse problem using smoothed cumulative PSD (Gomes et al., 2004; Ramkrishna, 2000). Gomes et al. (2004) showed that the statistical error is reduced when working with the cumulative distribution function to minimize the relative error in classes of larger size. On the other hand, cumulative distributions are usually used to reduce the measurement noise in the experimental data (Vikhansky, Kraft, Simon, Schmidt, & Bart, 2006). So, there is an obvious need to have the population balance equation written and solved in terms of the cumulative distribution function. The CQMOM described in Section 2, when applied to the PBE provides not only the cumulative number distribution, but also the required cumulative moments of higher order. To do this, multiply both sides of Eqs. (20)–(22) by ζ^r, replace each x by ζ, integrate with respect to $\zeta \in [0,x]$ and use the definition of the cumulative moments given by Eq. (2) to get the following integral form of the PBE:

$$\frac{\partial \mu_r(x;t)}{\partial t} + G(x;c)\frac{\partial(\mu_r(x;))}{\partial x} = r\int_0^x \zeta^{r-1}G(\zeta;c)w(\zeta;t)d\zeta + S_{b,r}(x) + S_{c,r}(x) \tag{23}$$

$$S_{b,r}(x) = -\int_0^x \zeta^r \Gamma(\zeta;\varphi)w(\zeta;t)d\zeta + \int_0^\infty \zeta^r\Gamma(\zeta;\varphi)w(\zeta;t)d\zeta \times \int_0^{\min(x,\zeta)} \left(\tfrac{x}{\zeta}\right)^r \beta(x|\zeta)dx \tag{24}$$

$$S_{c,r}(x) = \frac{1}{2}\int_0^x w(\zeta;t)d\zeta \int_0^{\eta(x,\zeta)} \psi(\zeta,u,\varphi)(u^3+\zeta^3)^{r/3}w(u;t)du - \int_0^x \zeta^r w(\zeta;t)d\zeta \int_0^\infty \psi(\zeta,u,\varphi)w(u;t)du \tag{25}$$

In the above derivation, the boundary condition $w(0;t)=0$ is utilized and note that $\partial\mu_r(x;t)/\partial x = x^r w(x;t)$. The above integral formulation of the PBE has several interesting properties that were highlighted individually in the literature. First, the left hand side of Eq. (23) is now in the standard Lagrangian form where the total derivative with respect to a moving reference frame is given by:

$$\frac{D\mu_r(x;t)}{Dt} = r\int_0^x \zeta^{r-1}G(\zeta;c)w(\zeta;t)d\zeta + S_{b,r}(x) + S_{c,r}(x) \tag{26}$$

The moving reference grid is now given by:

$$\frac{dx(t)}{dt} = G(x;c,t) \tag{27}$$

This is a desirable property of the present integral formulation, since the Lagrangian formulation does not result in a derivative source term like classical Lagrangian formulation of the PBE (see, e.g. reference Aamir, Nagy, Rielly, Kleinert, & Judat, 2009). Moreover, the above formulation is internally consistent to any desirable number of moments, which is a clear advantage when compared to the existing methods that are limited to a selected number of low-order moments (Aamir et al., 2009; Ramkrishna, 2000). This is because the classical QMOM is imbedded within the above formulation and is a special case when the limit of the particle size tends to infinity. The validity of the above integral equations at any given point x, facilitates the reconstruction of not only the

cumulative number distribution, but also the higher cumulative moments such as the mass cumulative distribution.

4. The discrete integral population balance equation

The integrals appearing in the source terms of Eqs. (23)–(25) can be evaluated using the cumulative quadratures developed in Section 2 since the nodes and weights of the Gauss–Christoffel quadrature are now continuous functions of the particle size x. The discrete form of the integral PBE is derived by first expanding the number concentration function as a sum of Dirac delta functions weighted by $\lambda_j(x;t)$ and located at $\zeta_j(x;t)$ as follows:

$$w(x;t) = \sum_{j=1}^{N_q} \lambda_j(x;t)\delta(\zeta - \zeta_j(x;t)) \tag{28}$$

By formal substitution of this expansion in Eqs. (24)–(26) and making use of the Dirac delta function properties, one gets the following semi-discrete form the integral PBE:

$$\frac{D\mu_r(x;t)}{\partial t} = r\sum_{j=1}^{N_q} \zeta_j^{r-1}(x;t)G(\zeta_j(x;t);c)\lambda_j(x;t) + S_{b,r}(x) + S_{c,r}(x) \tag{29}$$

$$\begin{aligned} S_{b,r}(x) = &-\sum_{j=1}^{N_q} \zeta_j^r(x;t)\Gamma(\zeta_j(x;t);\varphi)\lambda_j(x;t) \\ &+ \sum_{j=1}^{N_q} \zeta_j^r(x_\infty;t)\Gamma(\zeta_j(x_\infty;t);\varphi)\lambda_j(x_\infty;t) \\ &\times \int_0^{\min(x,\zeta_j)} \left(\frac{x}{\zeta_j}\right)^r \beta(x|\zeta_j)dx \end{aligned} \tag{30}$$

$$\begin{aligned} S_{c,r}(x) = &\frac{1}{2}\sum_{j=1}^{N_q}\sum_{n=1}^{N_q} \lambda_j(x;t)\lambda_n(\eta(x,\zeta_j);t)\Psi_{j,n,r}(x;t) \\ &- \sum_{j=1}^{N_q} \zeta_j^r(x)\lambda_j(x)\sum_{n=1}^{N_q} \lambda_n(x_\infty)\psi(\zeta_n(x),\zeta_n(x_\infty),\varphi) \end{aligned} \tag{31}$$

$$\Psi_{j,n,r}(x) = [\zeta_j^3(x) + \zeta_n^3(\eta(x,\zeta_j))]^{r/3}\psi(\zeta_n(\eta(x,\zeta_j)),\zeta_j(x),\varphi) \tag{32}$$

Note that the above system of equations has the same structure as that of the standard QMOM; however, at any arbitrary grid point x. This makes the present integral formulation numerically equivalent to the special case at $x = x_\infty$ (QMOM) in terms of computational cost.

To eliminate the finite domain error (error introduced by truncating the infinite domain of integration using a finite value of particle size: x_∞), x_∞ in the above equations is chosen as the minimum particle size at which $\lim_{x\to x_\infty} \partial\mu_r(x)/\partial x \approx \Delta\mu_r(x)/\Delta x \approx 0, \quad \forall r = 0, 1 \ldots 2N_q - 1$.

Note that, substitution of the quadrature nodes and weights given by Eqs. (11)–(14) or (16)–(18) closes the system of Eqs. (29) and (30), which now consists of $2N_q - 1$ equations (for this case $N_q = 2$). In addition, the above system of equations is continuous with the respect to the particle size x and can be sampled arbitrarily to reconstruct the first $2N_q - 1$ low-order cumulative moments of the number concentration function $w(x;t)$. To do this, let the particle size be discretized into M arbitrary grid points such that: x_i, $i = 1, 2 \ldots M$. Since the integral quantities in the source terms of the integral population balance equation are evaluated only at any given grid point x_i, and no information is needed at the other grid points (except for the source term of aggregation), the present numerical scheme is viewed as a mesh-free one. For the case of particle aggregation, information on the grid points x_m, $m = 1, 2, \ldots i$ is needed to evaluate the integral (see Eq. (25)):

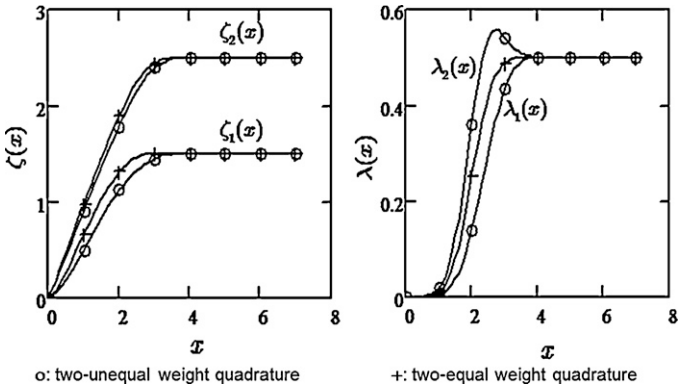

Fig. 2. Evolution of the two-weight quadrature nodes (left) and weights (right) along the particle size using Eqs. (11)–(14) and (16)–(18). The cumulative moments used in calculation are those of normal distribution function with mean and standard deviation equal to 2.0 and 0.5, respectively.

$$I_{j,i,r} = \int_0^{\min(x_i,\zeta_{j,i})} \psi(\zeta_{j,i}, u, \varphi)(u^3 + \zeta_{j,i}^3)^{r/3} w(u;t)du, \quad j = 1, 2, \ldots N_q \tag{33}$$

This is because no grid point (x_i, $i = 1, 2 \ldots M$) coincides exactly with the upper integral limit $\eta(x_i, u_j) = \sqrt[3]{x_i^3 - u_j^3}, \quad \forall j \in 1, 2 \ldots i$. In this case the quadrature nodes and weights (need at $\eta(x_i, u_j)$) are interpolated using the available ones at the grid points x_m, $m = 1, 2, \ldots i$. As can be seen from Fig. 2, although the variation of the quadrature nodes and weights along the particle size is quite steep at the small size range, it is found that a course particle size grid is enough for an accurate interpolation to get the missed quadrature's nodes and weights. Again, the two-equal weight quadrature is better in interpolating the missed weights due to the smooth variation of the weights when compared to the two-unequal weight quadrature (Fig. 3, left panel).

Finally, one gets the full discrete integral PBE by sampling $\mu_r(x;t)$ at the ith grid point ($x = x_i$):

$$\frac{D\mu_r(x_i;t)}{\partial t} = r\sum_{j=1}^{N_q} \zeta_j^{r-1}(x_i;t)G(\zeta_j(x_i;t);c)\lambda_j(x_i;t) + S_{b,r}(x_i) + S_{c,r}(x_i) \tag{34}$$

$$\begin{aligned} S_{b,r}(x_i) = &-\sum_{j=1}^{N_q} \zeta_j^r(v;t)\Gamma(\zeta_j(x_i;t);\varphi)\lambda_j(x_i;t) \\ &+ \sum_{j=1}^{N_q} \zeta_j^r(x_M;t)\Gamma(\zeta_j(x_M;t);\varphi)\lambda_j(x_M;t) \\ &\times \int_0^{\min(x_i,\zeta_j)} \left(\frac{x}{\zeta_j}\right)^r \beta(x|\zeta_j)dx \end{aligned} \tag{35}$$

$$S_{c,r}(x_i) = \frac{1}{2}\sum_{j=1}^{N_q}\sum_{n=1}^{N_q}\lambda_j(x_i;t)\lambda_n(\eta(x_i,\zeta_j);t)\Psi_{j,n,r}(x_i;t) - \sum_{j=1}^{N_q}\zeta_j^r(x_i)\lambda_j(x_i)\sum_{n=1}^{N_q}\lambda_n(x_M)\psi(\zeta_n(x),\zeta_n(x_M),\varphi) \quad (36)$$

Where $\Psi_{j,n,r}(x_i)$ is given by Eq. (32) evaluated at $x = x_i$ and x_M is chosen such that $[\mu_r(x_M) - \mu_r(x_{M-1})]/[x_M - x_{M-1}] \approx 0$, $\forall r = 0, 1 \ldots 2N_q - 1$.

Note that the structure of the discrete system given by Eqs. (34)–(36) is hierarchical and admits simplified, rapid and accurate solutions of the population balance equation. For example, using only one grid point the QMOM is recovered; however, without supplying any information about the distribution itself. By increasing the number of grid points and solving repeatedly the above system of ODEs M times, all the low-order cumulative moments are reconstructed with the desired accuracy. Here the accuracy of the reconstructed low-order moments at any given time is affected only by the number of quadrature points (N_q), since the reconstruction step is decoupled from the integration of the PBE over the particle size using the CQMOM.

5. Numerical results and discussion

In this section numerical results are presented and analyzed to illustrate the implementation of the CQMOM for particle growth. Cases for particle breakage, simultaneous and simultaneous particle growth and aggregation were presented separately (Attarakih & Bart, 2012; Attarakih et al., 2011). For the particle growth case, it is demonstrated by choosing spatially homogeneous PBE with growth laws for which analytical solutions are amenable. This does not restrict the generality of the present method, but it isolates the interaction of complex flow field numerical algorithms with the population balance solvers. For particle growth, two popular cases, which were tested in the literature are considered here; namely, particle diffusion limited growth and linear particle growth (Gimbun, Nagy, & Rielly, 2009; McGraw, 1997). These can be described by the general power law growth rate:

$$G(x) = G_0 x^p \quad (37)$$

When $p = 1$ and -1 we have linear and diffusion limited particle growth rates, respectively. The particle growth rate constant is taken as $G_0 = 0.78$ μm^2/s for particle diffusion limited growth (McGraw, 1997) and $G_0 = 0.02$ s^{-1} for the case of linear particle growth (Gimbun et al., 2009).

5.1. Case1: linear particle growth law

For the case of linear particle growth and in the absence of breakage and aggregation source terms, Eqs. (26) and (27) are closed in terms of the cumulative moments and are amenable to analytical solution by solving the cumulative moment ordinary differential equation:

$$\frac{D\mu_r(x;t)}{Dt} = rG_0\mu_r(x;t) \quad (38)$$

along the particle trajectories, which are solution of Eq. (27): $x(t) = x(0)e^{G_0 t}$. The formal solution of Eq. (38) along these trajectories is:

$$\mu_r(x;t) = \mu_r^0(\gamma(t)x)\left(\frac{1}{\gamma(t)}\right)^r, \quad \gamma(t) = e^{-G_0 t}, \quad r = 0, 1, \ldots \quad (39)$$

For this case and in the absence of breakage and aggregation source terms, the numerical solution of Eqs. (27) and (34) is accomplished using the explicit first-order Euler's method with step size $\Delta t = 0.1$ s:

$$\mu_r(x_i^{n+1}) = \mu_r(x_i^n) + \Delta t\sum_{j=1}^{N_q}\zeta_j^{r-1}(x_i^n)G(\zeta_j(x_i^n))\lambda_j(x_i^n), \quad r = 0, 1 \ldots 2N_q - 1 \quad (40)$$

$$x_i^{n+1} = x_i^n + \Delta t G(x_i^n) \quad (41)$$

where $n = 0, 1, \ldots N$, $N = (t_{final} - t_{initial})/\Delta t$ and the initial continuous particle trajectories are uniformly sampled according to the partition: $x_i(0)$, $i = 1, 2 \ldots M$, $M = (x_{\max} - x_{\min})/\Delta x$ with $x_{\min} = 0.001$ μm, $x_{\max} = 6$ μm and $M = 20$. The quadrature nodes and weights appearing in Eq. (40) are obtained from the two-unequal weight quadrature using Eqs. (1)–(14) or the two-equal weight quadrature given by Eqs. (16)–(18). Both quadratures give similar results for this case and the case of diffusion limited growth. So, only the results of the two equal-weight quadrature are presented here. Note that the discrete particle trajectories given by Eq. (41) grows exponentially as function of time for this special case and are deformed in general for an arbitrary growth law. In practice, the population balance equation is generally coupled to the continuous phase transport equations, which are normally solved in Eulerian reference frame using fixed grids. To exchange information between these mixed grids, the particle trajectories are projected on the fixed Eulerian grid. By making use of the present integral formulation, in which the population balance equation is written in terms of the monotone cumulative moments, monotone piecewise Hermite cubic interpolating polynomials (Fritsch & Carlson, 1980) are used to interpolate the solution on the course moving grid. These polynomials are well documented (Fritsch & Carlson, 1980; Kahaner, Moler, & Nash, 1989) and are programed in the standard built in MATLAB function *pchip*, which is used in the present numerical algorithm. This step is crucial and if the monotone nature of the data is not respected, nonphysical spurious oscillation might appear near sharp moving fronts, when it is interpolated. So, let the operator $CHerm(x)$ be the piecewise cubic Hermite interpolating polynomials and x_m^f, $m = 1, 2 \ldots L$ be a fixed grid of length L, then the cumulative moments on the moving grid (x^{n+1}) are projected back on the fixed grid (x^f) at each time step as follows:

$$\mu_r^{n+1}(x^f) = CHerm(x^{n+1}, \mu_r(x^{n+1}), x^f) \quad (42)$$

The initial condition for this case is taken as a normal distribution function with mean and standard deviations as 2.0 μm and 0.5 μm, respectively. The results obtained from the numerical scheme given by Eqs. (39)–(42) are shown in Figs. 3–6.

First, Fig. 3(a) shows the particle trajectories (solid lines) in the (t, x) plane where the particle size growing exponentially (according to Eq. (27)) in fixed grid environment (dotted lines). The monotone cumulative moments at $t = 50$ s are shown in Fig. 4 and are accurately projected on the fixed grid using the solution on the course grid given by these trajectories using the piecewise Hermite cubic interpolating polynomials as given by Eq. (42). Therefore, it is clear from Fig. 4 how the first low-order cumulative moments are accurately predicted when compared to the analytical solution given by Eq. (39). Note that the QMOM is recovered at the end point of the moving grid $x_M^{n+1} = 10$ μm, since the condition implied by Eq. (4) is always satisfied as shown in Fig. 4 because all the cumulative moments are constants for particle size greater than 7 μm approximately.

To reconstruct the differential number concentration ($w(x;t)$) from the cumulative zero moment ($\mu_0(x;t)$), one can use the identity $\partial\mu_0(x;t)/\partial x = w(x;t)$. However; accurate numerical evaluation

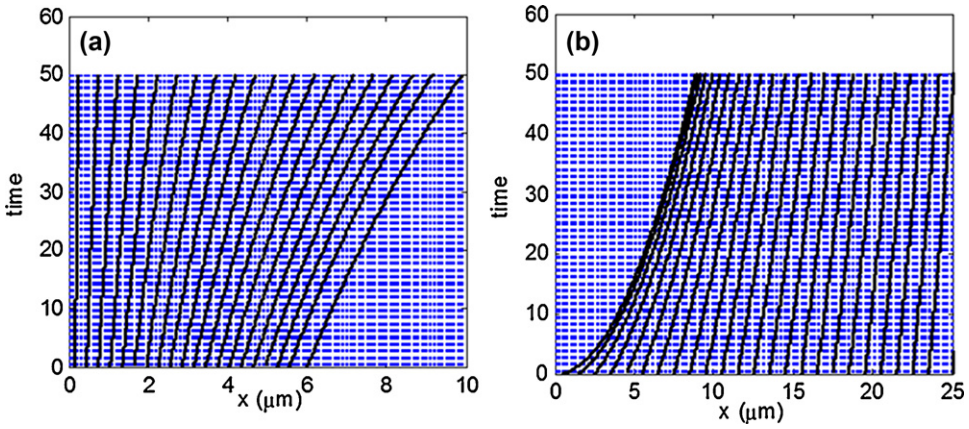

Fig. 3. Lagrangian moving grid (solid lines), which is superimposed on a fine fixed grid (dots) for monotone solution interpolation. (a) Linear particle growth rate. (b) Diffusion-limited particle growth rate.

of this derivative using second-order schemes might result in spurious oscillations near sharp fronts.

To avoid this problem, we devise a second-order nonoscillatory central difference scheme proposed by Kurganov and Tadmor using a one-parameter nonlinear monomod limiter (Kurganov & Tadmor, 2000):

$$w(x_i^n) = \frac{\partial \mu_0(x_i^n)}{\partial x} = \min \mathrm{mod}\left(\theta \frac{\mu_0(x_{i+1}^f) - \mu_0(x_i^f)}{\Delta x}, \frac{\mu_0(x_{i+1}^f) - \mu_0(x_{i-1}^f)}{2\Delta x}, \theta \frac{\mu_0(x_i^f) - \mu_0(x_{i-1}^f)}{\Delta x}\right) \tag{43}$$

Where $\theta \in [1, 2]$ and the multivariate minmod limiter is given by:

$$\min \mathrm{mod}(v_1, v_2, \ldots) = \begin{cases} \min\limits_j \{v_j\}, & \text{if } v_j > 0 \ \ \forall j \\ \max\limits_j \{v_j\}, & \text{if } v_j < 0 \ \ \forall j \\ 0, & \text{otherwise} \end{cases}$$

Note that the larger values of $\theta = 2$ corresponds to less dissipative, but in general, more oscillatory limiter. For values of $\theta = 1$ one gets first order one-sided differentiation formula with first order accuracy. The idea behind using limiters comes from the literature of computational fluid dynamics in solving hyperbolic conservation laws (Rosner et al., 2003). Second-order accurate methods such as central difference schemes for evaluating spatial derivatives give much better accuracy on smooth solutions than the first-order forward or backward methods. However; second-order methods fail near discontinuities, where oscillations are generated. In fact, even when the solution is smooth, oscillations may appear due to the dispersive nature of these methods. First-order methods have the advantage of keeping the solution monotonically varying in regions where the solution should be monotone, even though the accuracy is not very good. The idea behind the above minmod limiter is to combine the best features of both methods. Second-order accuracy is obtained where possible in smooth regions, while it is suppressed near sharp ones. So, it is clear now that the above minmod limiter combines first-order forward, backward and second-order central difference schemes. Accordingly, the minmod limiter given by Eq. (43) is used to construct the differential number concentration from the interpolated solution on the fixed grid.

The data of $\mu_0(x_i^f)$ shown in the first panel of Fig. 4 are now differentiated with the results shown in Fig. 5. It is clear that the number density function $w(x)$ is reconstructed with a very high accuracy (using only 40 grid points) when compared to the analytical solution, which is given by an expression similar to Eq. (39):

$$w(x;t) = \gamma(t) w_0(\gamma(t)x), \quad \gamma(t) = e^{-G_0 t} \tag{44}$$

Note that since the solution is smooth, a value of $\theta = 2$ is used in Eq. (43) to force the limiter to be second order accurate (Kurganov & Tadmor, 2000).

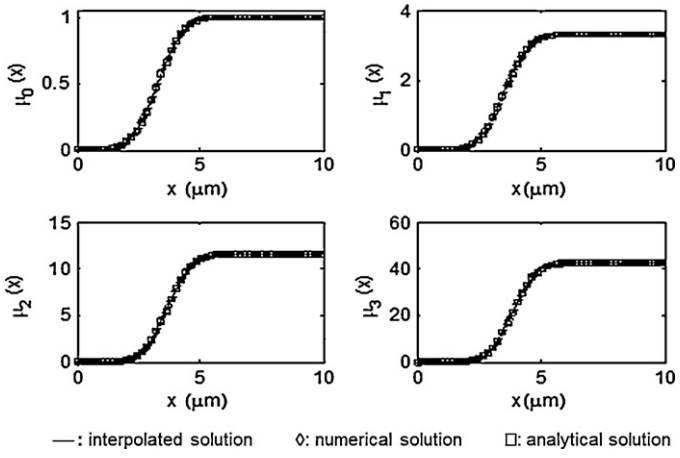

Fig. 4. Comparison between analytical and predicted cumulative distributions for particle linear growth at final time of 50 s. The number of grid points is 20 and the time step is 0.05 s with normal distribution initial condition: $\mu = 2$, $\sigma = 0.5$.

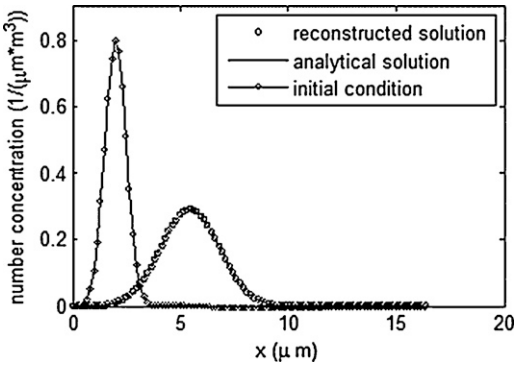

Fig. 5. Reconstructed number density function from the cumulative zero moment shown in Fig. 4 using the minmod limiter given by Eq. (43) with $\theta = 2$. The number of grid points is 40 and the time step is 0.05 s with normal distribution as an initial condition: $\mu = 2$, $\sigma = 0.5$.

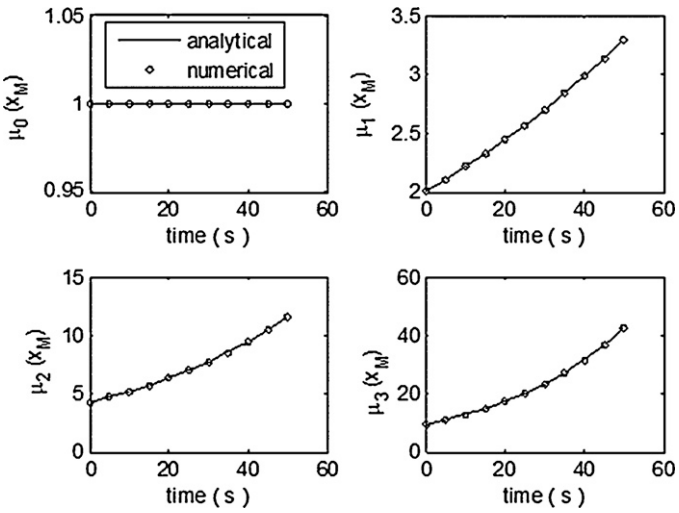

Fig. 6. Comparison between analytical (Eq. (40) with $x = x_M$) and predicted global moments for particle linear growth law at final time of 50 s. The number of grid points is 20 and the time step is 0.05 s with normal distribution as an initial condition: $\mu = 2, \sigma = 0.5$.

Fig. 6 shows the evolution of the first four low-order global moments as function of time as predicted by the CQMOM. The results show an excellent agreement between the analytical (Eq. (39) with $x = x_M$) and numerical solutions. Here the CQMOM is reduced exactly to the QMOM at $x = x_M$.

5.2. Case2: diffusion-limited particle growth law

This case study is taken from McGraw (1997) for diffusion-limited growth, which applies under conditions that the particle size is greater than the mean-free path of the gas. The growth law for this case is given by Eq. (39) with $p = -1$. The growth rate constant $G_0 = 0.78\ \mu m^2/s$ is for sulfuric acid – water droplets, where the particle size is taken here as droplet radius. The analytical solution for this case is derived in a similar way as that presented in McGraw (1997) and is given by:

$$\mu_r(x;t) = \int_0^{\sqrt{\max(0,x^2-2G_0t)}} [u^2 + 2G_0t]^{r/2} w_0(u)du \qquad (45)$$

First, the four low-order moments as predicted by the CQMOM are presented in Fig. 7 and compared to the analytical solution given by Eq. (45). Again as in case 1, the CQMOM predicts very accurately the cumulative low order moments along the particle radius. Note that Global moments ($\mu_r(x_M, t_f)$) at the final simulation time are recovered using the last grid point x_M. Here, the analytical solution is obtained by evaluating the integral appearing in Eq. (45) numerically using adaptive Gauss quadrature at any time and grid point.

To recover the differential number density function, the cumulative zero-order cumulative moment given in the first panel of Fig. 7 is differentiated using Eq. (43). The result is shown in Fig. 8 along with the particle weight and abscissa as function of grid points. Here the initial distribution is smooth function as shown in the upper panel of Fig. 8. However; after $t = 50$ s the particle diffusion-limited growth results in a discontinuity moving along the particle size as shown in the second panel of Fig. 8. The use of the minmod limiter (with $\theta = 1.7$) is necessary here to avoid spurious oscillations near the discontinuity, which develops along the particle size. Also, a fine grid is needed ($M = 100$) to capture this discontinuity. On the other hand, in the integral formulation this is not a requirement since the discontinuity is contained within the integration domain and no derivative is needed. This is a clear advantage of

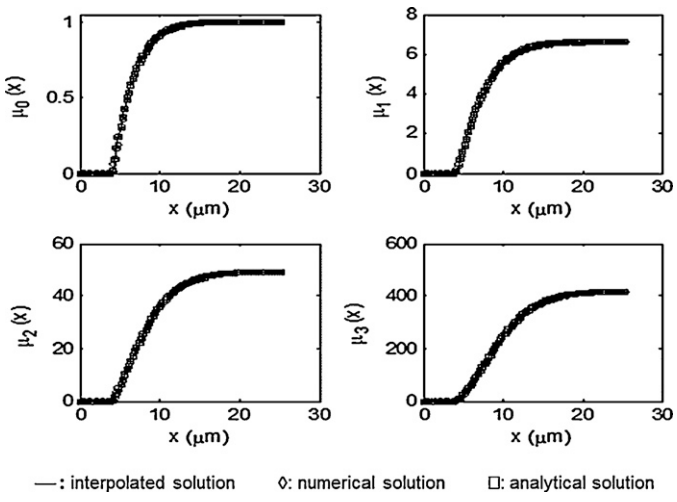

Fig. 7. Comparison between analytical and predicted cumulative distributions for a particle diffusion-limited growth at final time of 50 s. The number of grid points is 35 and the time step is 0.05 s with an initial condition as given by McGraw (1997).

the integral formulation of the PBE. In the lower panel of Fig. 8, the cumulative particle abscissa are shown as function of grid points. At the discontinuity point the number density function is an impulse and hence, the two abscissa are identical according to Eqs. (17) and (18). After the number density function start falling along the particle size, the two abscissa start departing from each other to reflect this change. It is worthwhile to mention here that the unequal-two weight quadrature given by Eqs. (11)–(14) fails here at the

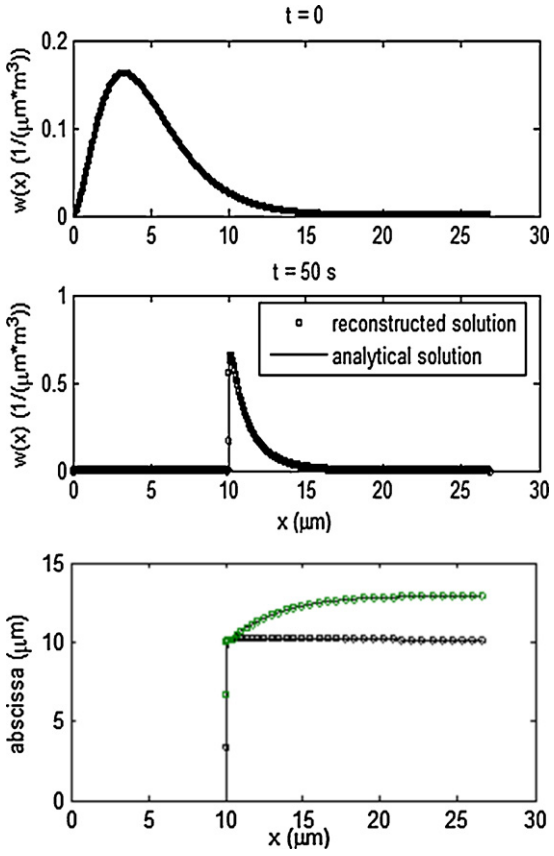

Fig. 8. Reconstructed number density function from the cumulative zero moment shown in Fig. 7 using the minmod limiter given by Eq. (43) with $\theta = 1.7$. The number of grid points is 100 and the time step is 0.05 s with an initial condition as given by McGraw (1997).

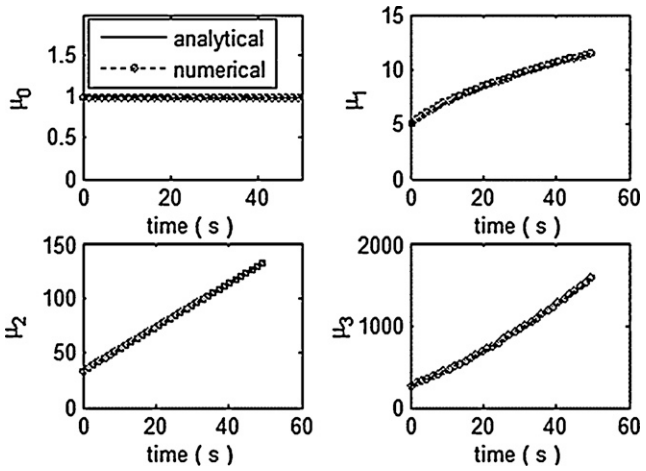

Fig. 9. Comparison between the analytical (McGraw, 1997) and predicted global moments for particle diffusion limited growth law at final time of 50 s. The number of grid points is 35 and the time step is 0.05 s with an initial condition as given by McGraw (1997).

discontinuity point as discussed in Section 2.1. For the case of linear particle growth rate (case 1), the two quadratures (equal and unequal weight) perform well since the number density function remain continuous as function of time (see Fig. 5).

The global moments of the particle size distribution as function of time are depicted in Fig. 9 at $x = x_M$. Actually, the analytical moments computed using Eq. (45) are not distinguishable from those predicted using the CQMOM, which are essentially the same as those calculated by McGraw (1997) using the QMOM.

To see the performance of the CQMOM, when the solution of the PBE is bimodal, a bimodal normal distribution function is chosen as an initial condition, which is shown in Fig. 10(a) for the case of diffusion-limited growth law. First, the two cumulative quadrature abscissa change along the particle size to reflect the bimodal form of the final solution as shown in the upper panel of Fig. 10(a). The cumulative number density function reproduces the exact bimodal form of the distribution as shown in the lower panel of Fig. 10(a). The number density function is also correctly reconstructed thanks to the minmod limiter given by Eq. (43). As can be seen the accuracy is remarkable, and the two solutions are in fact indistinguishable (the percentage relative error in the cumulative number density function is less than 0.035). It is worthwhile to mention here the simplicity and natural construction of the cumulative number density function and its low-order moments when compared to the recent reconstruction algorithm developed by John et al. (2007, 2010). In their work, the non-adaptive and adaptive cubic spline reconstruction is based on a very sophisticated algorithm (in terms of structure and implementation) when compared to the present straight forward and natural integral formulation of the PBE. For qualitative comparison, John et al. (2007, 2010) were able to reconstruct bimodal distributions with moderate accuracy using minimum four moments. They reported considerable sensitivity of the reconstructed solution to the number of the input moments, which had an error in the order of 35% for a case similar to that shown in Fig. 10. Moreover, inevitable negative oscillation around sharp points in the distribution was reported in their reconstruction due to the use of cubic splines as interpolating polynomials.

Finally, the CPU time requirement for solving the integral population balance equation using the CQMOM is compared to the SQMOM (Attarakih et al., 2009). A case study involving simultaneous particle breakage and aggregation (with constant frequencies) is simulated using a 3-point cumulative Gauss–Christoffel quadrature (Attarakih et al., 2011). The results are shown in Fig. 11 where the CPU dependence on the number

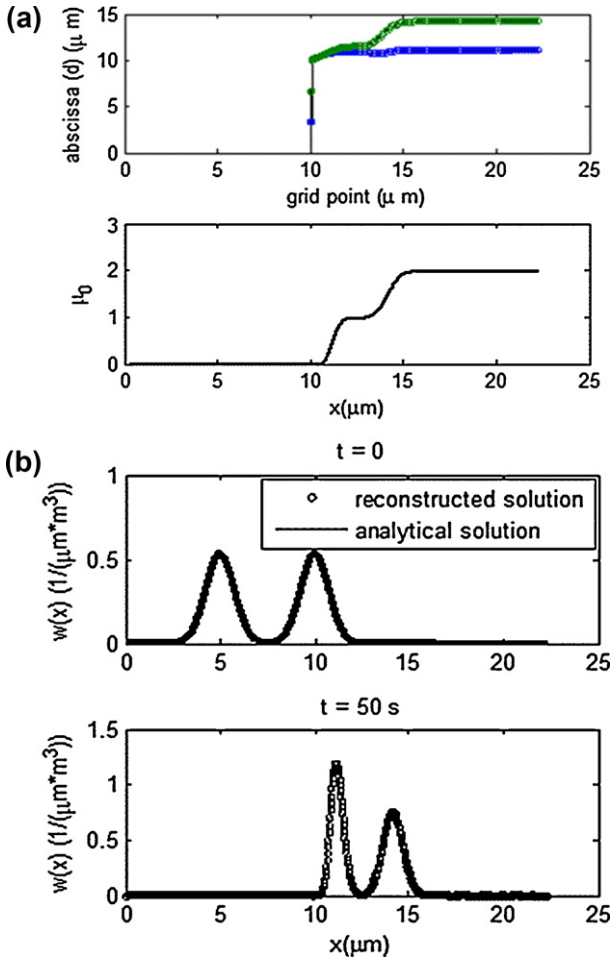

Fig. 10. (a) Variation of the cumulative quadrature weights (upper panel) and the cumulaitve zero-order moment (lower panel) along particle size. (b) Reconstructed number density function from the cumulative zero-order moment shown in (a) using the minmod limiter given by Eq. (43) with $\theta = 2$. The number of grid points is 100 and the time step is 0.05 s. The initial condition is a bimodal normal distribution shown in the upper panel with means: 5, 10 and standard deviation 0.75.

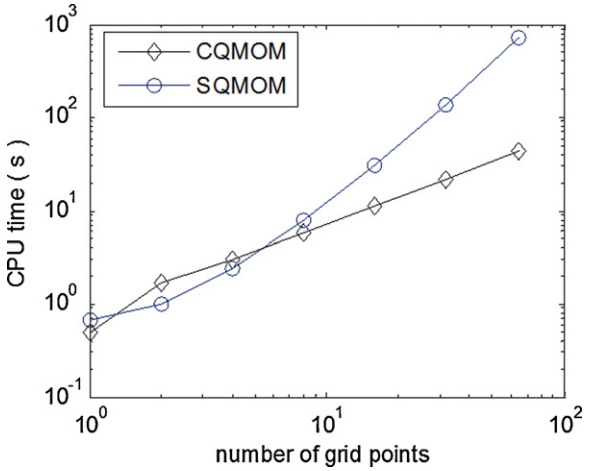

Fig. 11. Dependence of the CPU time on grid points for the case of simultaneous particle breakage and aggregation in batch vessel with constant breakage and aggregation frequencies. The number of quadrature points is 3 and the final simulation time is 5 units and a fixed-step size trapezoidal rule as an ODE solver with $\Delta t = 0.1$ is used. All the numerical experiments were carried out using Laptop with 1.8 GHz speed performing single task with MATLAB R2009a 32 bit.

of grid points is linear and much less than the SQMOM, especially when the number of grid points is greater than 10. This is because many double summations in the discrete source term of the SQMOM (especially for particle aggregation) are involved. It is worthwhile to mention here that the CPU time of executing numerical algorithms using MATLAB depends on vectorizing the code, where no rigorous optimization of the two algorithms is carried out. We believe accurate design and implementation of the above algorithms may result in reduced CPU time.

6. Summary and conclusions

In the present work a cumulative Gauss–Christoffel quadrature in terms of the low-order cumulative moments ($\mu_r(x;t)$) is derived and evaluated. The product difference algorithm (PDA) of Gordon (1968) is extended to accommodate continuous low-order cumulative moments in terms of particle property space. As special case of the PDA, the weights and abscissa of two-unequal weight cumulative quadrature are derived analytically. It is shown in this work that the cumulative weights and abscissa are positive at any given point in the particle property space and the quadrature nodes are symmetric about their mean. This cumulative quadrature conserves the total population mass when the particle internal property is chosen as a particle diameter. It has been shown that the cumulative weights are strongly coupled to the cumulative abscissa which makes this two-point quadrature, in particular and the PDA in general, collapse for monosize distributions or even unstable for very sharp distributions. To overcome this problem, the cumulative two-equal weight quadrature is derived and analyzed. The quadrature has two equal weights and each one of them equals to half the zero cumulative moment. The two abscissa are proved to be fluctuations of the particle size about its arithmetic mean, which results in symmetric quadrature nodes. The cumulative Gauss–Christoffel quadrature motivates the reformulation of the population balance equation in an integral form. This formulation is given the name Cumulative QMOM (CQMOM). This integral formulation of the population balance equation is guaranteed to reproduce exactly (from mathematical point of view) any desired number of low-order moments, and can handle discontinuous solutions of the population balance equation. In contrast to the QMOM which destroys the number density function, the present integral formulation produces not only the cumulative number density function, but also its low-order cumulative moments. When the differential number density function is required, then a monotone reconstruction method is introduced based on a one parameter nonoscillatory minmod limiter to recover the solution. For the case of particle growth, the hyperbolic system of integral equations with nonlinear source term is solved using a Lagrangian moving grid projected back on a fixed grid using monotone piecewise Hermite cubic interpolating polynomials. The moving grid structure is arbitrary and is decoupled from the accuracy of the quadrature approximation of the unclosed integrals. This makes the present method a mesh-free method and is reduced simply to the standard QMOM when only one grid point is placed at infinity. The accuracy of the method is tested against known analytical solutions, which are commonly encountered in the literature. The numerical results show an excellent agreement between the predicted and analytical solutions.

Compared to the SQMOM, the CQMOM is found superior in terms of CPU requirement especially when the number of grid points is greater than 10.

Acknowledgments

The author wish to acknowledge the Deutsche Forschungsgemeinschaft (DFG) for the financial support during his research stays in the summer time of the years 2009, 2010, 2011 and 2012 at the University of Kaiserslautern/Chair of Separation Science and Technology.

References

Aamir, E., Nagy, Z. K., Rielly, C. D., Kleinert, T., & Judat, B. (2009). Combined quadrature method of moments and method of characteristics approach for efficient solution of population balance models for dynamic modeling and crystal size distribution control of crystallization processes. *Industrial & Engineering Chemistry Research*, *48*, 8575–8584.

Abedini, H., & Shahrokhi, M. (2008). Inferential closed-loop control of particle size distribution for styrene emulsion polymerization. *Chemical Engineering Science*, *63*, 2378–2390.

Attarakih, M. (2010). System and method for simulating and modeling the distribution of discrete systems. *US Patent and Trademark Office (USPTO), Pub. No. US2010/0106467A1*. USA.

Attarakih, M. M., & Bart, H.-J. (2012). Integral formulation of the smoluchowski coagulation equation using the Cumulative Quadrature Method of Moments (CQMOM). *Computer Aided Chemical Engineering*, *31*, 1130–1134.

Attarakih, M., Bart, H.-J., & Faqir, N. (2006). Numerical solution of the bivariate population balance equation for the interacting hydrodynamics and mass transfer in liquid–liquid extraction columns. *Chemical Engineering Science*, *61*, 113–123.

Attarakih, M. M., Drumm, C., & Bart, H.-J. (2009). Solution of the population balance equation using the sectional quadrature method of moments (SQMOM). *Chemical Engineering Science*, *64*, 742–752.

Attarakih, M. M., Jaradat, M., Hlawitschka, M. W., & Bart, H.-J. (2011). Integral formulation of the population balance equation using the Cumulative Quadrature Method of Moments (CQMOM). *Computer Aided Chemical Engineering*, *29*, 81–85.

Bruns, M. C., & Ezekoye, O. A. Development of a hybrid sectional quadrature-based moment method for solving population balance equations. *Journal of Aerosol Science*, in press.

Cameron, I. T., Wang, F. Y., Immanuel, C. D., & Stepanek, F. (2005). Process systems modelling and applications in granulation: A review. *Chemical Engineering Science*, *60*, 3723–3750.

Chiu, T. Y., & Christofides, P. D. (2000). Robust control of particulate processes using uncertain population balances. *AIChE Journal*, *46*, 266–280.

Diemer, R. B., & Ehrman, S. H. (2005). Pipeline agglomerator design as a model test case. *Powder Technology*, *156*, 129–145.

Diemer, R. B., & Olson, J. H. (2002). A moment methodology for the coagulation and breakage problems: Part 2-moment models and distribution reconstruction. *Chemical Engineering Science*, *57*, 2211–2228.

Drumm, C., Attarakih, M., Hlawitschka, M. W., & Bart, H.-J. r. (2010). One-group reduced population balance model for CFD simulation of a pilot-plant extraction column. *Industrial & Engineering Chemistry Research*, *49*, 3442–3451.

Favero, J. L., & Lage, P. L. C. (2012). The dual-quadrature method of generalized moments using automatic integration packages. *Computers and Chemical Engineering*, *38*, 1–10.

Fox, R. O. (2008). A quadrature-based third-order moment method for dilute gas-particle flows. *Journal of Computational Physics*, *227*, 6313–6350.

Fox, R. (2009). Optimal moment sets for multivariate direct quadrature method of moments. *Industrial & Engineering Chemistry Research*, *48*, 9686–9696.

Fritsch, F. N., & Carlson, R. E. (1980). Monotone piecewise cubic interpolation. *SIAM Journal on Numerical Analysis*, *17*, 238–246.

Gautschi, W. (1968). Construction of Gauss–Christoffel quadrature formulas. *Mathematics of Computation*, *22*, 251–270.

Gelbard, F., & Seinfeld, J. (1980). Simulation of multicomponent aerosol dynamics. *Journal of Colloid and Interface Science*, *78*(2), 485–501.

Gimbun, J., Nagy, Z. K., & Rielly, C. D. (2009). Simultaneous quadrature method of moments for the solution of population balance equations, using a differential algebraic equation framework. *Industrial & Engineering Chemistry Research*, *48*, 7798–7812.

Gomes, L. N., Guimares, M. L., Lopes, J. C., Madureira, C. N., Stichlmair, J., & Cruz-Pinto, J. J. (2004). Reproducibility of the hydrodynamic performance and measurements in a liquid–liquid Kuhni extraction columns relevance to theoretical model evaluation. *Industrial & Engineering Chemistry Research*, *43*, 1061–1070.

Gordon, R. G. (1968). Error bounds in equilibrium statistical mechanics. *Journal of Mathematical Physics*, *9*, 655–663.

Grosch, R., Briesen, H., Marquardt, W., & Wulkow, M. (2007). Generalization and numerical investigation of QMOM. *AIChE Journal*, *53*, 207–227.

Hamilton, R. A., Curits, J. S., & Ramkrishna, D. (2003). Beyond log-normal distributions: Hermite spectra for solving population balances. *AIChE Journal*, *49*, 2328–2343.

Hjortso, M. A. (2004). *Population balances in biomedical engineering*. The McGraw-Hill Companies.

Hulburt, H. M., & Katz, S. (1964). Some problems in particle technology. *Chemical Engineering Science*, *19*, 555–574.

Isaacson, E., & Keller, H. B. (1994). *Analysis of numerical methods*. New York: Dover Publications, Inc.

John, V., Angelov, I., Öncülc, A. A., & Thévenin, D. (2007). Techniques for the reconstruction of a distribution from a finite number of its moments. *Chemical Engineering Science*, *62*, 2890–2904.

John, V., Angelov, I., Öncülc, A. A., & Thévenin, D. (2010). Techniques for the reconstruction of a distribution from a finite number of its moments. *Chemical Engineering Science*, *65*, 2741–2750.

Kahaner, D., Moler, C., & Nash, S. (1989). *Numerical methods and software*. New Jersey: Prentice Hall.

Kumar, S., & Ramkrishna, D. (1996). On the solution of population balance equations by discretization—I. A fixed pivot technique. *Chemical Engineering Science*, *51*, 1311–1332.

Kurganov, A., & Tadmor, E. (2000). New high-resolution central schemes for nonlinear conservation laws and convective diffusion equations. *Journal of Computational Physics*, *160*, 241–282.

Lage, P. L. C. (2011). On the representation of QMOM as a weighted-residual method—The dual-quadrature method of generalized moments. *Computers and Chemical Engineering*, *35*, 2186–2203.

Majumder, A., Kariwala, V., Ansumali, S., & Rajendran, A. (2010). Fast high-resolution method for solving multidimensional population balances in crystallization. *Industrial & Engineering Chemistry Research*, *49*, 3862–3872.

Majumder, A., Kariwala, V., Ansumali, S., & Rajendran, A. (2012a). Lattice Boltzmann method for multi-dimensional population balance models in crystallization. *Chemical Engineering Science*, *70*, 121–134.

Majumder, A., Kariwala, V., Ansumali, S., & Rajendran, A. (2012b). Lattice Boltzmann method for population balance equations with simultaneous growth, nucleation, aggregation and breakage. *Chemical Engineering Science*, *69*, 316–328.

Marchisio, D. L., & Fox, R. O. (2005). Solution of population balance equations using the direct quadrature method of moments. *Journal of Aerosol Science*, *36*, 43–73.

McGraw, R. (1997). Description of aerosol dynamics by the quadrature method of moments. *Aerosol Science and Technology*, *27*, 255–265.

Mickler, M., Didas, S., Jaradat, M., Attarakih, M., & Bart, H.-J. (2011). Tropfenschwarmanalytik mittels Bildverarbeitung zur Simulation von Extraktionskolonnen mit Populationsbilanzen. *Chemie Ingenieur Technik*, *83*, 226–237.

Mnatsakanov, R. M., & Hakobyan, A. S. (2009). Recovery of distributions via moments. *IMS Lecture Notes – Monograph Series*, *57*, 252–265.

Motz, S., Mitrovic, A., & Gilles, E.-D. (2002). Comparison of numerical methods for the simulation of dispersed phase systems. *Chemical Engineering Science*, *57*, 4329–4344.

Piskunov, V. N., & Golubev, A. I. (2002). The generalized approximation method for modeling coagulation kinetics – Part 1: Justification and implementation of method. *Journal of Aerosol Science*, *33*, 51–63.

Raikar, N. B., Bhatia, S. R., Malone, M. F., & Henson, M. A. (2006). Self-similar inverse population balance modeling for turbulently prepared batch emulsions Sensitivity to measurement errors. *Chemical Engineering Science*, *61*, 7421–7435.

Ramkrishna, D. (2000). *Population balances: Theory and applications to particulate systems in engineering*. San Diego: Academic Press.

Rosner, D. E. (2006). Improved rate laws and population balance simulation methods: CRE applications including the combustion synthesis of valuable nano-particles. *International Journal of Chemical Reactor Engineering*, *4*, 1–11.

Rosner, D. E., McGraw, R., & Tandon, P. (2003). Multivariate population balances via moment and Monte Carlo simulation methods: An important sol reaction engineering bivariate example and "mixed" moments for the estimation of deposition, scavenging, and optical properties for populations of nonspherical suspended particles. *Industrial & Engineering Chemistry Research*, *42*, 2699–2711.

Sasvari, Z. (1994). *Positive definite and definitizable functions*. Akademie Verlag.

Schmidt, S. A., Simon, M., Attarakih, M. M. G., & Bart, L. L. H.-J. (2006). Droplet population balance modeling—Hydrodynamics and mass transfer. *Chemical Engineering Science*, *61*, 246–256.

Smooke, M., McEnally, C., Pfefferle, L., Hall, R., & Colket, M. (1999). Computational and experimental study of soot formation in a coflow, laminar diffusion flame. *Combustion and Flame*, *117*(1–2), 117–139.

Strumendo, M., & Arastoopour, H. (2006). Solution of PBE by MOM in finite size domains. *Chemical Engineering Science*, *63*, 2624–2640.

Strumendo, M., & Arastoopour, H. (2009). Solution of bivariate population balance equations using the finite size domain complete set of trial Functions Method of Moments (FCMOM). *Industrial & Engineering Chemistry Research*, *48*, 262–273.

Su, J., Gu, Z., Li, Y., Feng, S., & Xu, X. Y. (2008). An adaptive direct quadrature method of moment for population balance equations. *AIChE Journal*, *54*, 2872–2887.

Tiwari, S., Drumm, C., Attarakih, M. M., Kuhnert, J., & Bart, H.-J. (2008). Coupling of the CFD and the Droplet population balance equation with finite poinset method. In M. Griebel, & M. A. Schweitzer (Eds.), *Lecture notes in computational science and engineering: Meshfree methods for partial differential equations IV* (pp. 315–334). Springer Verlag.

Vikhansky, A., Kraft, M., Simon, M., Schmidt, S., & Bart, H.-J. (2006). Droplets population balance in a rotating disc contactor: An inverse problem approach. *American Institute Chemical Engineering Journal*, *52*, 1441–1450.

Wang, T., & Wang, J. (2007). Numerical simulations of gas–liquid mass transfer in bubble columns with a CFD–PBM coupled model. *Chemical Engineering Science*, *62*, 7107–7118.

Xiong, Y., & Pratsinis, S. E. (1993). Formation of agglomerate particles by coagulation and sintering—Part I. A two-dimensional solution of the population balance equation. *Journal of Aerosol Science*, *24*, 283–300.